Cyclic Interplanetary Motion of a Cargo Solar Sail

Miroslav A. Rozhkov[a,**], Olga L. Starinova[a]

[a] Flight Dynamics and Control Theory Department, Samara National Research University, Samara, Russia

Abstract

Future of mankind lies in a Mars colonization and exploiting resources floating in our Solar system. Solar sails can become a key technology to provide that future with constant flow of materials to Earth and from it. We propose applying a solar sail to ensure cyclic heliocentric motion of a cargo spacecraft between Earth and inner planets. The work investigates following ballistic aspects of the suggested transport system: cyclic motion dynamics and numerical simulation that considers non-ideally reflecting surface of a solar sail and optical parameters degradation; heliocentric trajectory optimization by minimum time criterion. As a prototype spacecraft for the simulation, we use a design from work [1] that can carry 1905 kg of payload with 0.25 mm/s^2 acceleration. Applying Pontryagin's maximum principle we define Hamiltonian and solve the boundary value problem with consideration of non-ideal reflection and degradation. The simulation is carried out for 4 loops of cyclic motion Earth-Mars-Earth to demonstrate a possibility of the suggested transport system. Results show that the degradation causes an increase of flight time for 4 cycles up to 14 years. Despite that the system can be efficient with deployment of several cargo spacecrafts with solar sail to maintain a flow of material with shorter periods

Keywords: cargo solar sail, cyclic space motion, optical degradation, interplanetary flight, trajectory optimization

Nomenclature

a	Acceleration
A	Solar sail area
r	Heliocentric distance
u	Angular coordinate
V	Velocity
ω	Angular velocity
c	Speed of light
S_r	Solar irradiance at distance r
m	Spacecraft mass
θ	Solar radiation incidence angle (control)
ρ	Reflectivity
ς	Specular reflection factor
ε	Emissivity
B	non-Lambertian coefficient
p	Optical parameter
d	Degradation factor
λ	Degradation coefficient
Σ	Solar radiation dose
T	Time period
δ	Angular distance between planets
U	A set of possible control
H	Hamiltonian
ψ	Costate variable
r	Position vector
V	Velocity vector
X	State vector
D	Design parameters vector
ψ	Costate vector

Superscripts
*	Optimal

Subscripts
$\perp$	Perpendicular to sail's surface
$\parallel$	In sail's surface plane
fr	Sail's front side
b	Sail's back side
yr	One year time
0	Initial
f	Final
r	Radial component
u	Transverse component
p	Target planet
∞	Optical parameter at maximum degradation
i	ith interplanetary flight

1. Introduction

Interplanetary flights require significant energy costs, including a launch of a spacecraft from the Earth's surface to a departure trajectory, deceleration after

---
* Corresponding author, rozhkov.ma@ssau.ru

spacecraft enters a sphere of influence of a target planet, and landing. Thus, when designing a transport system that ensures the movement of cargo between two planets of the Solar System, traditional launch vehicles will have to spend their resources on delivering not only a payload, but also a fuel that will be consumed in an intermediate heliocentric and planetocentric flight stages. To increase a mass efficiency of transport interplanetary missions, it is proposed to use intermediate interplanetary transport spacecraft [2,3].

In Russia, nuclear electric rocket propulsion tugs have been suggested as prospective reusable transport vehicles [3], which possess high efficiency and autonomy. Another alternative is the use of an orbital station located away from the planet on which the spacecraft performs refueling. The fuel itself is planned to be extracted or produced directly in space. This concept is followed by NASA in its Deep Space Transport project [2], where the lunar orbital station (Lunar Gateway) [4], which is situated in the Earth-Moon halo orbit, serves as a port for refueling and cargo transfer.

This work discusses the possibility of an alternative variant of such a transportation system that applies solar sails capabilities of not consuming any fuel. A large-area reflective thin film is capable of providing a small but constant acceleration to the spacecraft through the pressure of solar electromagnetic radiation [5,6]. The feasibility of deploying large thin-film systems has been demonstrated by spacecraft such as Znamya-2 [7,8], *IKAROS* [9], *LightSail-2* [10], etc. Possibilities of using them for cargo delivery have been analyzed in [8,9].

Solar sails yield lower thrust compared to other propulsion systems, which increases the duration of mission. However, with a large number of interplanetary flights performed, their utilization becomes justified. Naturally, the trajectory along which the spacecraft moves must ensure minimal flight time requirement.

Such trajectories have been explored in the study [12], but the authors assumed a constant orientation of the sail relative to the Sun, considered phases of the spacecraft's passive orbiting at the Lagrange points, and applied direct optimization methods. In this dissertation, the Pontryagin's maximum principle is used for calculating nominal control programs, allowing for obtaining an optimal program of sail attitude control and the corresponding trajectory that satisfies the optimality criterion.

A schematic representation of the proposed transportation system's operation is presented in Fig. 1. One cycle of movement consists of two interplanetary flights.

Designing a transportation system that facilitates the transfer of cargo to a solar sail is an important part of the proposed method for interplanetary cargo delivery and requires separate investigation. Such a transportation system may involve a spacecraft with an electric propulsion engine [13]. However, a detailed analysis of it is beyond the scope of this work. The issues related to delivering the transport spacecraft with the solar sail from the surface of the Earth and deploying the sail are also not considered.
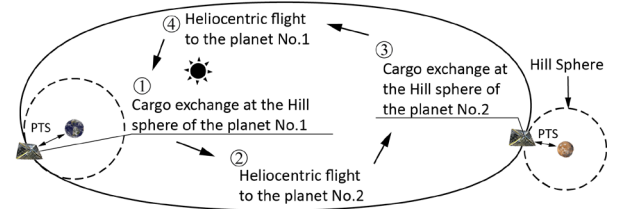
Fig. 1. Scheme of one cycle motion between two planets along heliocentric trajectory. The cargo delivery from solar sail at Hill Sphere to planet or orbital station is performed by planetary transport system (PTS).

For the ballistic scheme of a transport mission, the movement of the spacecraft with the solar sail is primarily influenced by the gravitational field of the Sun, with only minor perturbations from the planets at the beginning and end of the trajectory. Therefore, mathematical models and calculations for planetocentric segments are not included in this dissertation, which significantly simplifies the optimization process.

2. Mathematical Models

In order to evaluate a possibility of such motion we need to address a problem of optical parameters influence on the solar sail dynamics [14]. While searching for the optimal cyclic trajectory incorrect mathematical description of solar sail operation can lead to incorrect assumption of sail's abilities to execute the suggested cargo transportation system. In the paper we consider a non-ideally reflecting solar sail mathematical model and a degradation of front surface optical parameters.

2.1. Non-ideally reflecting solar sail

The acceleration of a spacecraft with a flat non-ideal reflective solar sail due to the pressure of electromagnetic radiation can be defined as the sum of two components directed normal ($a_\perp$) and parallel ($a_{||}$) to the sail surface in the plane passing through the radius vector:

$$a_\perp = 2\frac{S_r}{cm} A \cdot \cos\theta \cdot (a_1 \cos\theta + a_2), \qquad (1)$$

$$a_{||} = -2\frac{S_r}{cm} A \cdot \cos\theta \cdot a_3 \sin\theta, \qquad (2)$$

where

$$a_1 = \frac{1}{2}(1 + \varsigma\rho), \quad a_3 = \frac{1}{2}(1 - \varsigma\rho),$$

$$a_2 = \frac{1}{2}\left(B_f(1-\varsigma)\rho + (1-\rho)\frac{\varepsilon_f B_f - \varepsilon_b B_b}{\varepsilon_f + \varepsilon_b}\right).$$

Forward's optical model of the grey solar sail includes six different optical parameters, however only 3 of them, that are related to the sail's front surface, will be changing due to degradation.

When selecting $\rho = 1$ and $\varsigma = 1$ the Eq. (2) gives zero and Eq. (1) correspond to the model of ideally-reflecting solar sail where acceleration directs along the normal to sail's surface. We will use such conditions in order to get an initial guess for optimal trajectory. In addition, it allows to compare how non-ideal reflection and degradation influence dynamics of the solar sail cyclic motion.

The grey solar sail model also helps with the controlling through incident angle instead of cone angle. That simplifies the optimal control problem and gives some practical meaning since one can use sun sensors to realize calculated optimal control program. Hence it is useful for control system design.

There are many other things to consider that allows getting more accurate calculation of the generated acceleration: wrinkles, shape curvature and solar irradiance uncertainties, etc. All them that stacks together and may influence significantly in the real flight. However, in the scope of calculating nominal control program and optimal trajectory design it is rationally to consider only non-ideally reflecting and degradation.

2.2. Optical Parameters Degradation

The surface of the sail degrades during the flight due to the influence of various space factors. In particular, the reflectivity coefficient worsens, leading to an increased fraction of absorbed radiation. In the work [15], the authors propose a parametric model to describe the degradation process of the solar sail.

The model consists of a system of three equations that determine the ratio of the current value of one of the optical parameters $p(t)$ to its initial value p_0:

$$\frac{p(t)}{p_0} = \begin{cases} \dfrac{1 + d e^{-\lambda\Sigma(t)}}{1+d} & if\ p \in \{\rho, \varsigma\}, \\ 1 + d\left(1 - e^{-\lambda\Sigma(t)}\right) & if\ p = \varepsilon_f, \\ 1 & if\ p \in \{\varepsilon_b, B_f, B_b\}. \end{cases} \quad (3)$$

The dimensionless radiation dose $\Sigma(t)$ is calculated as the ratio of the received radiation dose $\tilde{\Sigma}(t)$

accumulated by the sail during the flight to the total dose $\tilde{\Sigma}_0 = 15.768 \cdot 10^{12}$ TJ/m^2 received by a surface with an area of 1 m^2 at a distance of 1 AU over the course of one year.

$$\Sigma(t) = \frac{\tilde{\Sigma}(t)}{\tilde{\Sigma}_0} = \frac{1}{T_{yr}}\int_{t_0}^{t}\frac{\cos\theta(t)}{r^2}dt. \quad (4)$$

The degradation coefficient determines the intensity of degradation, and its mathematical description corresponds to half of the time of the sail's maximum degradation:

$$\lambda = \frac{\ln 2}{\hat{\Sigma}}. \quad (5)$$

Degradation factor d defines optical parameters values at which their change with time becomes infinitely low $\lim\limits_{t\to\infty} p(t) = p_\infty$:

$$\rho_\infty = \frac{\rho_0}{1+d}, \quad \varsigma_\infty = \frac{\varsigma_0}{1+d}, \quad \varepsilon_{f\infty} = \varepsilon_{f0}(1+d). \quad (6)$$

2.3. Equation of Motion

The results of studies on the calculation of trajectories for spacecraft with solar sails have shown that even the most simplified model of the sail and its orbital motion provides sufficient results for the evaluation and prediction of interplanetary flight trajectories [6,16–18]. It can be used as an initial approximation for the optimization and modeling of more complex models of the spacecraft's motion with a solar sail. Therefore, a mathematical model of flat heliocentric motion of the spacecraft is used for assessing the dynamics of cyclic sail motion and optimizing control. In the paper, following assumptions are made:

- Planar motion is considered.
- Perturbations from celestial objects are not taken into account.
- The intensity of solar radiation varies inversely with the square of the distance and does not change over time (independent of solar activity).
- Planetary orbits are assumed to be circular and lying in the plane of the ecliptic.

To describe the motion of the spacecraft, a system of differential equations of motion in a planar polar coordinate system (Fig. 2) is used in dimensionless form.

$$\frac{d\mathbf{r}}{dt} = \mathbf{V}, \quad \frac{d\mathbf{r}}{dt} = \mathbf{a}(r,\theta,\Sigma) - \frac{\mathbf{r}}{\mathbf{r}^3}, \quad \frac{d\Sigma}{dt} = \frac{1}{T_{yr}}\frac{\cos\theta}{r^2}. \quad (7)$$

The coordinates, velocity components, and accelerations in Eq. (7) are dimensionless and scaled with respect to the radius of the Earth's orbit, its circular velocity, and the centripetal acceleration.
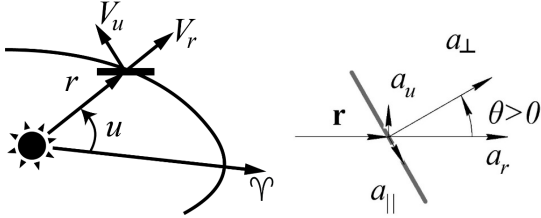
Fig. 2. Directions of vectors components in the plane polar coordinate system.

Scalar values of acceleration components in the planar polar coordinate system are calculated using the solar sail's installation angle θ, which serves as the control angle, through a rotation matrix in two-dimensional space.

$$a_r = a_\perp \cos\theta - a_{||} \sin\theta,$$
$$a_u = a_\perp \sin\theta + a_{||} \cos\theta. \tag{8}$$

In the scales of interplanetary flights, the difference in distances from the Sun and orbital velocities between the planet and points on the boundary of the Hill sphere is less than 1%. In this case, phase coordinates of the departure and destination planets can be used as boundary conditions for interplanetary flights. The initial values of the spacecraft's phase coordinates are determined by the previous stages of the flight, while the final value of accumulated radiation dose Σ_f is not fixed:

$$t = t_{i-1}, \quad \mathbf{X}_{0,i} = \{r_{f,i-1}, u_{f,i-1}, V_{f,i-1}, V_{f,i-1}, \Sigma_{f,i-1}\}^T,$$
$$t = t_{i-1} + T_i, \quad \mathbf{X}_{f,i} = \{r_{f,i}, u_{f,i}, V_{f,i}, V_{f,i}, \Sigma_{f,i} - unfix.\}^T. \tag{9}$$

The duration and angular distance of the flight should ensure that the angular motion of the destination planet and the spacecraft are equal.

$$\left\{\frac{u}{2\pi}\right\} = \left\{\frac{u_p + \omega_p T}{2\pi}\right\}. \tag{10}$$

where {.} denotes the operation of extracting the fractional part.

It is assumed that during cargo transfer, the sail is oriented edge-on to the Sun and does not generate thrust, while the spacecraft itself undergoes passive motion and awaits docking. In this study, the time required for cargo transfer was not considered in the calculations, as it does not affect the optimization algorithm of nominal control

but only changes the angular distance between the planets at the start of the heliocentric transfer.

3. Optimization

3.1. Optimization Problem Statement

Let's consider the initial angular distance between the planets δ_0 as a ballistic parameter of the optimization problem. The criterion for the optimality of cyclic trajectories is the flight time for the given design parameters of the spacecraft with the sail (mass, optical parameters, and sail area). The control of the sail through the sail angle θ has a constraint: the electromagnetic radiation pressure cannot act in the direction opposite to the radiation source.

The problem of ballistic optimization of cyclic trajectories based on time efficiency is formulated as follows: determine the nominal control function (where U is the set of admissible controls) and the initial angular distance between the departure and destination planets δ_0 (corresponding to the departure date) that minimize the total travel time and satisfy the boundary conditions Eq. (9) and rendezvous conditions Eq. (10) when given the design parameter vector of the spacecraft $\mathbf{D} = \{m, A, \rho_0, \varsigma_0, \varepsilon_{fr_0}, \varepsilon_b, B_{fr}, B_b\}^T$:

$$t_f^* = \min_{\theta(t), \delta_0} t_f \left(\theta(t), \delta_0 | D = fixed, \theta(t) \in U,\right.$$
$$\left. \mathbf{X}_0 = \mathbf{X}(t_0), \mathbf{X}_f = \mathbf{X}(t_f)\right). \tag{11}$$

For the considered in the paper transportation system, there are no waiting periods (passive motion of the spacecraft on the initial orbit), which determines the dependence of the initial phase coordinates of the current interplanetary flight $\mathbf{X}_{0,i}$ on the angular distance between the departure and destination planets at the end of the previous $\delta_{f,i-1}$. Based on this, it is assumed that the choice of δ_0 in the first cycle determines the subsequent optimal cyclic trajectory, which consists of individually optimized interplanetary flights based on minimum time criterion. For a given number of cycles n, it is possible to find a value δ_0^* that minimizes the total duration of the entire cyclic heliocentric trajectory by minimizing the duration of each individual interplanetary trajectory:

$$T_i^* = \min_{\theta(t)} T_i \left(\theta(t) | \mathbf{D} = fixed, \theta(t) \in U, \delta_{0,i} = \delta_{f,i-1},\right.$$
$$\left. \mathbf{X}_{0,i} = \mathbf{X}(t_{i-1}), \mathbf{X}_{f,i} = \mathbf{X}(t_{i-1} + T_i)\right). \tag{11}$$

3.2. Optimal Control Program

The solution to the optimization problem of the nominal control program for spacecraft motion with an ideally reflecting sail, based on the criterion of minimizing the flight duration, is well known and has been obtained using the Pontryagin's maximum principle by the authors of paper [19].

$$\tan\theta = \frac{\sqrt{9\psi_{Vr}^2 + 8\psi_{Vu}^2} - 3\psi_{Vr}}{4\psi_{Vu}}. \tag{12}$$

The Pontryagin's maximum principle provides a necessary condition for optimality: if a trajectory is optimal, then the value of the Hamiltonian reaches a maximum. To find the optimal control program, the first derivative of the Hamiltonian with respect to the sail installation angle θ is calculated and set equal to zero.

$$\frac{\partial H}{\partial \theta} = \frac{a_c}{r^2}\psi_{Vr}\left(a_3\sin^3\theta + 2(a_1+a_2)\sin\theta\cos\theta - \right.$$

$$-\left(3a_1+2a_3\right)\cos^2\theta\sin\theta\right) + \frac{a_c}{r^2}\psi_{Vu}\left(\cos^3\theta - \right.$$

$$-2\sin^2\theta\left(a_2+\cos\theta\right)+a_2\right) - \frac{\cos\theta}{T_{yr}r^2}\psi_{\Sigma} = 0. \tag{13}$$

Analytical solution to determine the optimal angle θ from the Eq. (13) is hardly obtainable. Moreover, it is necessary to determine the sign of the second derivative with respect to the angle θ to establish whether the found extremum is a maximum. Therefore, in the study, the maximum of the Hamiltonian with respect to the control variable is numerically searched for at each step of simulating the spacecraft's motion using the golden section method.

3.3. Boundary Value Problem

To formulate the boundary value problem conclusively, a system of differential equations for the costate variables is defined. This system consists of the following equations:

$$\frac{\partial\boldsymbol{\psi}_r}{\partial t} = -\frac{\partial H}{\partial\mathbf{r}}, \frac{\partial\boldsymbol{\psi}_V}{\partial t} = -\frac{\partial H}{\partial\mathbf{V}}, \frac{\partial\psi_{\Sigma}}{\partial t} = -\frac{\partial H}{\partial\Sigma}. \tag{14}$$

To normalize the problem, $\psi_r(t_0)$ is taken to be ±1. From the results of similar works [20], it is known that a negative value corresponds to a decrease in the orbit radius, while a positive value corresponds to an increase. The subsequent calculation results in this study also confirmed this statement.

Thus, the variational problem reduces to a four-parameter boundary value problem, where it is necessary to find initial values of the costate variables $\boldsymbol{\psi}(t_0)$ that satisfy the boundary conditions.

For the numerical solution of the boundary value problem, a modified Newton's method with automatic convergence estimation and adjustment of step size for computing derivatives and constraints is used [20]. However, boundary value problems with a fixed angular distance converge poorly and require the application of additional methods to find an initial approximation. A sequential complexity increase method and descent along the parameter of the initial angular distance between the planets are employed.

Initially, the boundary value problem with an unfixed angular distance is solved i.e., the problem of spacecraft transfer from the initial to the target orbit. Such problems converge quickly, and their solution corresponds to satisfying the boundary condition of Eq. (10) (rendezvous mission) for the start date with the minimum transfer time and optimal planet positions.

The solution of the problem with the unfixed angular distance serves as a starting point for solutions along the parameter of the initial angular position of the planets. By solving boundary value problems with a fixed angular distance according to Eq. (10), a set of solutions can be obtained over the entire range of angular planet positions.

The obtained results are further used as a reliable close approximation for calculating the cyclic motion of the spacecraft with a non-ideally reflecting degrading sail. Thus, by forming two sets of solutions for the transfer from one planet to another and back, it is possible to determine trajectories for the spacecraft's motion along a cyclic trajectory.

Fig. 3 presents the results of Earth-to-Mars transfer calculations for a solar sail with a characteristic acceleration of 0.25 mm/s^2 and ideal reflection. The calculations were performed sequentially for the entire range of possible planet positions relative to each other, $\delta_0 = [0,360]$ deg. Two types of control programs are shown: sail orientation edge-on to the Sun ($\theta = \pm90$ deg.) at the end of the trajectory (for $\delta_0 = 145$ deg.) and at the beginning (for $\delta_0 = 340$ deg.).

The obtained results demonstrate a common pattern in the control programs. The solar sail tends to orient itself relative to the Sun at an angle of $\theta = \pm35$ deg. for the fastest change in the transverse component of velocity V_u. If the departure date is different from the optimal (in this case $\delta_0 = 159$ deg.), a synchronization stage takes place, i.e., a change in the final value of the angular distance to reach the target planet. Synchronization can occur at the beginning or end of the trajectory. The trajectories have a multi-turn spiral shape, which is typical for low-thrust spacecraft.
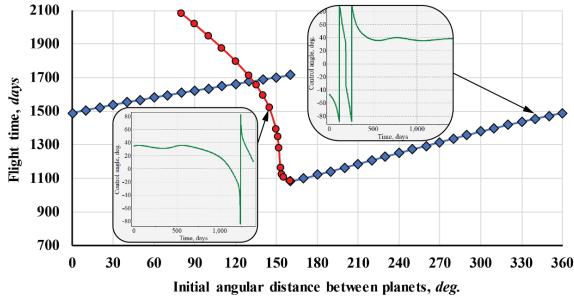
Fig. 3. The dependence of Earth-to-Mars transfer durations on the angular position of the planets. Two types of sail control programs are presented: ● – synchronization occurs at the beginning of the trajectory, ♦ – at the end.

The trajectories can exhibit non-monotonic changes in the heliocentric distance. This occurs during the synchronization stage, where the goal is to adjust the angular heliocentric velocity of the spacecraft and satisfy the boundary condition of Eq. (10) more quickly.

4. Earth-Mars-Earth Cyclic Motion Simulation

The design and optical parameters of the spacecraft with a solar sail are taken from references [1] and [21] and are showed in Table 1.

The threshold value for the reflectance coefficient, below which the film no longer degrades, is chosen as the value for low-carbon unpolished steel ($\rho_\infty = 0.32$) [22]. This allows obtaining parameters necessary for modeling degradation processes according to Eq. (6).

With these degradation parameters, the optical characteristics of the sail will deteriorate by 50% after 35 years of orbital motion around the Earth with perpendicular orientation to the Sun. Taking into account that modern technologies usually become obsolete morally after 20 years, the sail has a sufficient degradation lifespan to compete with existing propulsion systems in space and be economically viable for long-duration space missions. These results are consistent with the findings from MISSE 1 and MISSE 2 experiments [22].

As it was mentioned before in section 3.3 of this paper, it is necessary to generate a set of solutions for the entire range of possible planet positions relative to each other. The database for the Earth-Mars transfer was previously presented in Fig. 3. The solutions for the Mars-Earth transfer are shown in Fig. 4.

The calculation results are presented in Table 2. Fig. 5 shows the control programs for the 3rd and 4th cycles of the Earth-Mars transfer using both ideal and non-ideal reflecting solar sail. The Earth-Mars transfer trajectories for the 3rd cycle are shown in Fig. 6. The degradation of the optical parameters of the solar sail throughout all 4 cycles of the cyclic motion is depicted in Fig. 7.

Table 1. Design and optical parameters of the solar sail.

Parameter description and units		Value
Spacecraft mass, kg		2353
Cargo mass, kg		1905
Sail area, m2		75625
Characteristic acceleration, mm/s2		0.25
Reflectivity		0.91
Specular reflection factor		0.94
Emissivity	Front	0.05
	Back	0.55
non-Lambertian coefficients	Front	0.79
	Back	0.55
Degradation factor		1.75
Degradation coefficient		0.02
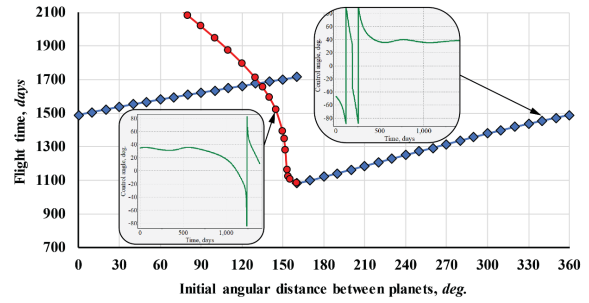
Fig. 4. The dependence of Mars-to-Earth transfer durations on the angular position of the planets.

Table 2. Flight time of interplanetary flights for 4 cycle of Earth-Mars-Earth cyclic motion.

Cycle	Flight time, years			
	Ideal sail		Non-ideal sail	
	to Mars	to Earth	to Mars	to Earth
I	2.96	3.16	3.58	5.00
II	3.23	3.18	4.11	4.62
III	3.23	3.18	6.29	4.52
IV	3.23	3.18	5.78	5.03

The optimal control program for an ideal reflecting sail, without degradation, is calculated in such way that the spacecraft performs cyclic motion with a constant cycle time. However, a non-ideal reflecting sail, due to degradation, is unable to maintain such stable motion. Nevertheless, the control program itself aims to minimize the possible variation in interplanetary transfer time.

a)

b)
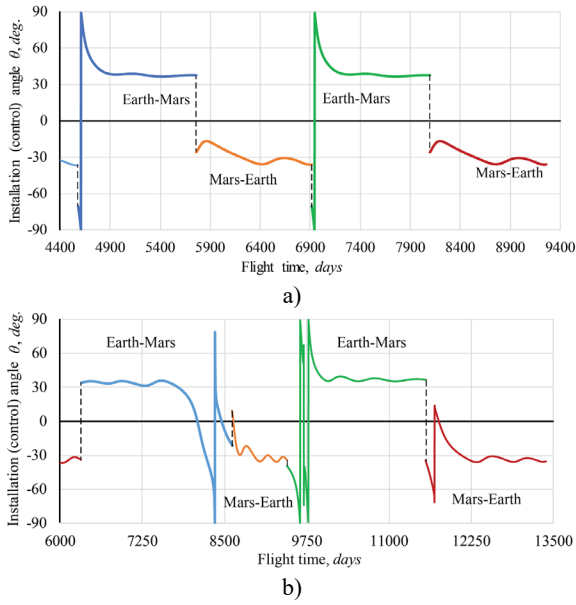
Fig. 5. Nominal control program during 3rd and 4th cycles of motion for a) ideally reflecting and b) non-ideally reflecting solar sail that undergoes degradation.

a)

b)
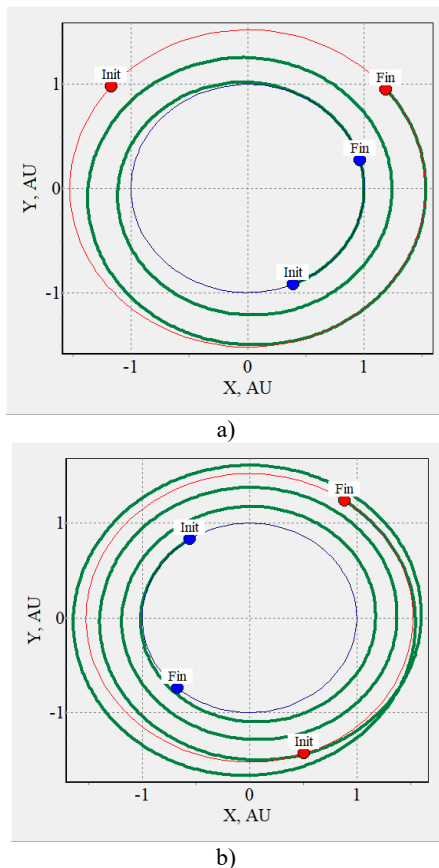
Fig. 6. Earth-Mars heliocentric trajectory of the 3rd cycle for a) ideally reflecting and b) non-ideally reflecting solar sail.
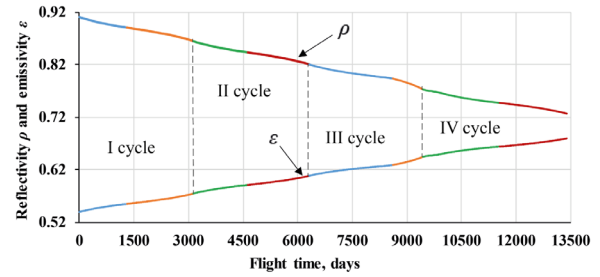
Fig. 7. Change of the solar sail's optical parameters with time throughout all 4 cycles of motion along Earth-Mars-Earth cyclic trajectory. Parameter ς is not shown since it has similar dependence as ρ with different initial value.

Another feature of the control program for a degrading, non-ideally reflecting sail is the selection of a trajectory for synchronizing the spacecraft's angular position with the target planet. The control is designed in such a way that synchronization occurs at the farthest distance from the Sun to reduce the received radiation dose. This holds true for all cycles except the fourth cycle, which is the final one. In this case, the control program may allow the spacecraft to descend closer to the Sun to quickly align its angular position since there is no need to preserve optical parameters for the last cycle.

5. Conclusion

The calculations of the heliocentric motion for the four cycles of Earth-Mars-Earth motion using a solar sail with a characteristic acceleration of 0.25 mm/s² were obtained. The travel time for an ideally reflecting solar sail along the cyclic Earth-Mars-Earth trajectories amounts to 6.4 years, and the total time for completing the four cycles is 25 years. However, in reality, due to the degradation of the sail's reflecting surface and considering the non-ideal reflection of electromagnetic radiation, the time for completing each cycle will inevitably vary. As a result, the minimum travel time for the four cycles amounts to 39 years.

The main challenge in accounting for solar sail degradation lies in determining the characteristics of the degradation process, namely, determining the degradation coefficient and factor. Ground-based facilities exist that can simulate material degradation processes in space [23], and there are even integrations with setups for measuring electromagnetic radiation pressure [24].

The economic feasibility of using a solar sail as a transportation system requires a comprehensive analysis of the expenses for design, assembly, launch, and operation. The considered interplanetary transportation system assumes that the solar sail leaves cargo and retrieves new cargo in the vicinity of a Lagrange point,

which means that the costs of a transportation system delivering cargo to the planet, orbital station, or natural satellite need to be taken into account as well.

References

[1] G.W. Hughes, M. Macdonald, C.R. McInnes, A. Atzei, P. Falkner. Sample Return from Mercury and Other Terrestrial Planets Using Solar Sail Propulsion, *Journal of Spacecraft and Rockets,* 43(2006): 828–835. https://doi.org/10.2514/1.15889.

[2] J.C. Crusan, R.M. Smith, D.A. Craig, J.M. Caram, J. Guidi, M. Gates, J.M. Krezel, N.B. Herrmann, Deep space gateway concept: Extending human presence into cislunar space. Big Sky, MT, USA, June 2018. IEEE Aerospace Conference Proceedings. doi.org/10.1109/AERO.2018.8396541.

[3] V. V Sinyavskii, Advanced technology for nuclear electric propulsion orbital transfer vehicle Hercules, *Kosm. Tekh. Tekhnol.* 3 (2013) 25–45.

[4] T.D. Haws, J.S. Zimmerman, M.E. Fuller, SLS, the Gateway, and a Lunar Outpost in the Early 2030s, in: IEEE Aerospace Conference Proceedings, IEEE Computer Society, 2019. https://doi.org/10.1109/AERO.2019.8741598.

[5] C.R. McInnes, *Solar sailing: technology, dynamics and mission applications*, Springer Berlin, Heidelberg, 2004.

[6] G. Vulpetti, L. Johnson, G.L. Matloff, *Solar sails: A novel approach to interplanetary travel*, 2nd ed., Springer New York, 2015. https://doi.org/10.1007/978-1-4939-0941-4.

[7] V.M. Melnikov, V.A. Koshelev, *Large Space Structures Formed by Centrifugal Forces*, CRC Press, 1998. https://doi.org/10.1201/9781003078203.

[8] V.M. Melnikov, K.M. Pichkhadze, Design of frameless SA deployed by centrifugal forces and its deployment mechanism as a basis of new technology of in-orbit power plant assembling, in: American Institute of Aeronautics and Astronautics (AIAA), 2005. https://doi.org/10.2514/6.iac-05-c2.p.01.

[9] O. Mori, H. Sawada, R. Funase, M. Morimoto, T. Endo, T. Yamamoto, Y. Tsuda, Y. Kawakatsu, J. Kawaguchi, Y. Miyazaki, Y. Shirasawa, I. Demonstration Team and Solar Sail Working Group, First Solar Power Sail Demonstration by IKAROS, *Transactions of The Japan Society for Aeronautical and Space Sciences*, Aerospace Technology Japan. 8 (2010) 25–31. https://doi.org/10.2322/tastj.8.To_4_25.

[10] D.A. Spencer, B. Betts, J.M. Bellardo, A. Diaz, B. Plante, J.R. Mansell, The LightSail 2 solar sailing technology demonstration, *Advances in Space Research*. 67 (2021) 2878–2889. https://doi.org/10.1016/j.asr.2020.06.029.

[11] R.H. Frisbee, Solar Sails for Mars Cargo Missions, AIP Conference Proceedings. 374 (2007) 374–380. https://doi.org/10.1063/1.1449747.

[12] M. Vergaaij, J. Heiligers, Time-optimal solar sail heteroclinic-like connections for an Earth-Mars cycler, *Acta Astronautica*. 152 (2018) 474–485. https://doi.org/10.1016/j.actaastro.2018.08.008.

[13] C. Du, O.L. Starinova, Y. Liu, Transfer between the planar Lyapunov orbits around the Earth–Moon L2 point using low-thrust engine, *Acta Astronautica*. 201 (2022) 513–525. https://doi.org/10.1016/j.actaastro.2022.09.056.

[14] M.A. Rozhkov, O.L. Starinova, I. V. Chernyakina, Influence of optical parameters on a solar sail motion, *Advances in Space Research*. 67 (2021) 2757–2766. https://doi.org/10.1016/j.asr.2020.06.017.

[15] B. Dachwald, G. Mengali, A.A. Quarta, M. Macdonald, Parametric model and optimal control of solar sails with optical degradation, *Journal of Guidance, Control, and Dynamics*. 29 (2006) 1170–1178. https://doi.org/10.2514/1.20313.

[16] M. MacDonald, *Advances in Solar Sailing*, Springer Science & Business Media, 2014. https://doi.org/10.1007/978-3-642-34907-2.

[17] R.Y. Kezerashvili, Space exploration with a solar sail coated by materials that undergo thermal desorption, *Acta Astronautica*. 117 (2015) 231–237. https://doi.org/10.1016/j.actaastro.2015.08.007.

[18] G. Vulpetti, Fast Solar Sailing, in: *Fast Solar Sailing*, Springer, Dordrecht, 2013: pp. E1–E2. https://doi.org/10.1007/978-94-007-4777-7_10.

[19] V.N. Lebedev, A.N. Zhukov, Variational problem of the transfer between heliocentric circular orbits by means of a solar sail, *translated from Kosmicheskie Issledovaniya (Cosmic Research)* (1964) 45-50.

[20] V. V. Salmin, O.L. Starinova, Optimization of interplanetary flights of spacecraft with low-thrust engines taking into account the ellipticity and noncoplanarity of planetary orbits, *Cosmic Research*. 39 (2001) 46–54. https://doi.org/10.1023/A:1002835811494.

[21] J.L. Wright, *Space sailing,* Gordon and Breach Science Publishers, 1992.

[22] J.A. Dever, S.K. Miller, E.A. Sechkar, T.N. Wittberg, Space Environment Exposure of Polymer Films on the Materials International Space Station Experiment: Results from MISSE 1 and MISSE 2, *High Performance Polymers*. 20 (2008) 371–387. https://doi.org/10.1177/0954008308089704.

[23] M. Sznajder, T. Renger, A. Witzke, U. Geppert, R. Thornagel, Design and performance of a vacuum-UV simulator for material testing under space conditions, *Advances in Space Research*. 52 (2013) 1993–2005. https://doi.org/10.1016/J.ASR.2013.08.010.

[24] N. Melnik, U. Geppert, B. Biering, F. Lura, Light Pressure Measurement at DLR Bremen, in: *Advances in Solar Sailing*. (2014) 399–406. https://doi.org/10.1007/978-3-642-34907-2_26.